

# Ultrasonography and contrast-enhanced CT findings of tularemia in the neck

Serap Doğan  
Afra Ekinci  
Hayati Demiraslan  
Ayşegül Ulu Kılıç  
Ertuğrul Mavili  
Mustafa Öztürk  
Hakan İmamoğlu  
Mehmet Doğanay

## PURPOSE

We aimed to evaluate the ultrasonography (US) and contrast-enhanced computed tomography (CECT) findings of tularemia in the neck.

## METHODS

US and CECT findings of 58 patients with serologically proven tularemia were retrospectively evaluated. Forty-eight patients underwent US and 42 patients underwent CECT. Lymph node characteristics and parotid preauricular region involvement were analyzed using US and CECT. In addition, involvement of larynx, oropharynx, and retropharynx; presence of periorbital edema; and neck abscess formation were evaluated using CECT. Fine needle aspiration cytology (FNAC) results of enlarged lymph nodes were analyzed in 29 patients.

## RESULTS

Hypoechoic pattern, round shape, absence of hilum, and cystic necrosis were seen in most of the lymph nodes especially at level 2 and 3 on US and CECT. Matting was more commonly observed than irregular nodal border on US and CECT. Parotid preauricular region involvement was seen in 20.8% of patients on US. Oropharyngeal, retropharyngeal, laryngeal and parotid preauricular region involvement and periorbital edema were seen in 52.4%, 19.1%, 4.8%, 31%, and 9.5% of tularemia patients, respectively. Neck abscess was found in 59.5% of patients on CECT. Suppurative inflammation was the most common finding of FNAC.

## CONCLUSION

Tularemia should be considered in the presence of level 2 and 3 lymph nodes with cystic necrosis, matting, absence of calcification, oropharyngeal and retropharyngeal region involvement, and neck abscess, particularly in endemic areas.

**T**ularemia is an acute bacterial zoonosis caused by *Francisella tularensis*, a noncapsulated, gram-negative coccobacillus (1). This bacterium was first isolated from rodents in 1911 in Tulare County, California, USA (2). Tularemia is classically more commonly seen in North America, Scandinavia, Japan, and Russia. In Sweden and Finland, tularemia outbreaks were occasionally reported. In addition, large epidemics have been previously reported in Spain, Kosovo, and Austria (3). In Turkey, tularemia epidemics were reported in different regions, such as Thrace Region, southern and northwestern parts of Turkey (namely, Antalya and Bursa), and Black Sea Region in 1945, 1953, 1988, and 2004, respectively (4). An increasing number of tularemia cases have been seen in Central Anatolia Region since 2009.

*F. tularensis* is a highly virulent pathogen capable of causing an infection even when present in small numbers (10–50 bacteria). It is considered a potential biologic weapon (5). *F. tularensis* should be studied at biosafety level 3 laboratories to prevent accidental exposure of the laboratory personnel. Rodents, rabbits, and hares are the main reservoirs of the bacteria. Humans may acquire this pathogen through several routes. Contact with an infected animal or their infectious tissues and fluids; a bite from an infected tick, deerfly, or mosquito; ingestion of contaminated water or food; and inhalation of infected aerosols are different ways of transmission (6). Clinical symptoms mainly depend on the port of entry into humans. Six different clinical forms of tularemia (ulceroglandular, glandular, oropharyngeal, oculoglandular, typhoidal, and pneumonic) have been described (7). The most common clinical presentation is ulceroglandular form, which has been frequently reported in endemic areas. In a retrospective study from 41 centers in Turkey, the most frequent clinical presentations were oropharyngeal

From the Departments of Radiology (S.D. ✉ [drserapdogan@hotmail.com](mailto:drserapdogan@hotmail.com), A.E, E.M., M.Ö. H.İ.), and Infectious Diseases and Clinical Microbiology (H.D., A.U.K., M.D.), Erciyes University School of Medicine, Kayseri, Turkey.

Received 27 January 2016; revision requested 27 February 2016; revision received 9 March 2016; accepted 14 March 2016.

Published online 05 August 2016.  
DOI 10.5152/dir.2016.16037

(85.3%), followed by glandular (13.1%), and oculoglandular (10.1%) forms (8).

Of patients with tularemia, 11%–45% have symptoms or signs localized in the head and neck region (9). Because of the nonspecific symptoms and clinical findings of the disease, such as fever, sore throat, fatigue, cough, myalgia, exudative tonsillopharyngitis, and cervical lymphadenomegaly (LAM), diagnosis of tularemia is usually delayed. Abscess rates are higher in patients with a delayed treatment. Patients diagnosed early can be treated with antibiotherapy before abscess formation. Antibiotherapy is often unsuccessful in patients with abscess and surgical drainage may be required. Generally, the awareness of tularemia is increased during outbreaks, but due to its rarity, it is not frequently cited in the differential diagnosis of cervical lymphadenopathy and abscess.

The diagnosis of tularemia is primarily based on clinical suspicion and serologic methods. Antibodies against the bacteria can be determined using agglutination or ELISA. There is little information about the imaging findings of tularemia, which is mostly limited to ultrasonography (US) findings. In this study, we investigated the US and contrast-enhanced computed tomography (CECT) findings of tularemia in the neck, which might raise suspicion of tularemia in the differential diagnosis.

## Methods

The present study was a retrospective single institutional study. It was approved by the institutional review board. We reviewed medical records of 58 consecutive patients (32 male, 26 female; mean age,

43.55 years; age range, 12–75 years) with serologically proven tularemia between January 2010 and January 2014. Tularemia was diagnosed in patients with clinical findings and symptoms suggestive of tularemia and the existence of specific antibody titers of  $\geq 1:160$  or at least a four-fold increase of antibody titer in two serum samples taken two weeks apart. The micro-agglutination tests were performed at the Public Health Reference Laboratory. Clinical presentations of patients were noted (10).

Picture archiving and communication system and medical reports were used for the evaluation of CECT and US findings. Of 58 patients, 48 underwent US and 42 underwent CECT. Results of US-guided fine needle aspiration cytology (FNAC) of enlarged lymph nodes in 29 patients were also analyzed.

### Ultrasonography

Neck US examinations were performed using a 7.5 MHz linear transducer (XU Xario, Toshiba). The US examination records were analyzed in terms of LAM and parotid preauricular region involvement. Extension of the inflammatory soft tissue into the parotid gland and edema were defined as parotid preauricular involvement.

### Contrast-enhanced CT

CECT scans were performed with a 16-slice spiral CT (Light-Speed 16, General Electric Medical System) with the parameters of: 120 kV, 140 mA, pitch 1, and 1.25 mm slice thickness, 0.8 s exposure time per rotation. The coverage of the neck CT was extended from skull base to the thoracic inlet. Iopromide 300 mg I/mL (Ultravist; Bayer Schering Pharma) was used as the contrast agent. It was administered via the antecubital vein using a Medrad Vistron CT injection system (Bayer) at a flow rate of 2.5 mL/s. The dose of contrast agent was 1–2 mL/kg. The CECT images were evaluated in terms of LAM; involvement of larynx, oropharyngeal, retropharyngeal, and parotid preauricular region; and presence of periorbital edema. Involvement of these structures was defined as obliteration of fatty planes and soft tissue swelling. Retropharyngeal lymph node and retropharyngeal abscess formation were also noted. Moreover, neck abscess was described as low-density area with peripheral rim enhancement, with the presence of mass effect and obliterated fatty planes on CECT (11).

### Lymph node characterization

Features including size, shape, presence of echogenic hilum, border, and internal structure of the lymph node were evaluated. Lymph nodes measuring more than 10 mm in the short axis diameter and containing one of the three features, (round shape, absence of echogenic hilum, and necrosis), were considered as involvement and included in the study.

The shape of the lymph node was determined by the short/long axis ratio (S/L) on a transverse plane. An S/L ratio of less than 0.5 was considered to be a long or oval node, whereas an S/L ratio of 0.5 or more was considered to be a round node (12). Hilum was defined by the presence or absence of hilar echogenicity on US and hilar hypodensity that is continuous with the surrounding fat on CECT. The border of the lymph node was classified as sharp or irregular according to the boundary between lymph nodes and the surrounding tissues. The internal structure of the lymph node was evaluated for calcification and cystic necrosis. Cystic necrosis was defined as an echolucent area within the nodes on US and a focal low attenuating area on CECT images (13, 14). The echo pattern of the lymph node was classified on US as hypoechoic, isoechoic, or hyperechoic compared with the surrounding musculature. In addition, matting and zonal distribution of lymph nodes were noted. Matting was defined as the confluence of multiple enlarged lymph nodes with absence of soft tissue normally seen between them. The largest lymph node was analyzed in each patient.

### Statistical analysis

Descriptive statistics were presented as frequency and percentages. The chi-square test was used for the comparison of two qualitative variables. Between groups, variables without normal distribution were compared using the Mann-Whitney U test. A *P* value of  $<0.05$  was considered to be significant.

## Results

The most frequent clinical presentation was oropharyngeal tularemia ( $n=31$ , 53.4%) followed by glandular ( $n=20$ , 34.4%) and oculoglandular tularemia ( $n=7$ , 12%). The mean duration of the symptoms was 40 days (3 days to 6 months).

### Main points

- Tularemia is a rare bacterial zoonosis. Diagnosis of tularemia is usually delayed because of the nonspecific symptoms and clinical findings of the disease. Patients diagnosed early can be treated with antibiotics alone, without surgery.
- Imaging features of cervical lymph node involvement in tularemia patients can be similar with malignant and tuberculous lymph nodes.
- Tularemia should be considered in the presence of level 2 and level 3 lymph nodes with cystic necrosis, matting, absence of calcification, oropharyngeal and retropharyngeal involvement, and neck abscess, particularly in endemic areas.

**Table 1.** Number of patients with lymph node involvement in the neck

	n (%)
Level 1	8 (13.7)
Level 2	52 (89.6)
Level 3	36 (62)
Level 4	5 (8.6)
Level 5	5 (8.6)
Data are presented as n (%).	

Level 2 was the most frequently involved neck site (n=52, 89.6%; Table 1). Bilateral nodal involvement was seen in 17% patients.

The mean short axis and long axis of lymph nodes were 21.5 mm (range, 10–50 mm) and 31.1 mm (range, 13–50 mm), respectively, on US. Lymph node features such as shape, hilum, border, cystic necrosis, and matting are summarized in Table 2 and examples are given in Figs. 1–3. Hypoechoic and isoechoic patterns were found in 93.7% (n=45) and 6.2% (n=3) of the lymph nodes, respectively. There was no calcification in lymph nodes on US. Parotid preauricular region involvement was seen in 20.8% (n=10) of patients on US examination.

The mean short axis and long axis of lymph nodes were 26.8 mm (range, 15–50 mm) and 34.3 mm (range, 16–70 mm) on CECT respectively. Lymph node features on CECT are shown in Table 3. Oropharyngeal, retropharyngeal, laryngeal, parotid preauricular region, and periorbital involvement frequencies are summarized in Table 4 (Figs. 4, 5). Laryngeal involvement was seen as epiglottic edema in two patients on CECT. There was no calcification in lymph nodes on CECT. Neck abscess was found in 59.5% (n=25) of the 42 patients on CECT. Abscess formation was more common in patients whose duration of symptoms was longer than three weeks ( $P < 0.05$ ).

Of the 29 patients who underwent FNAC, 21 (72.4%) were detected as having suppurative inflammation. Multinucleated giant cells and granuloma formation were seen in four (13.7%) and five (17%) patients, respectively. Cytologic findings of four (13.7%) cases were consistent with reactive lymphoid hyperplasia. Three aspirates (10.3%) were inadequate for assessment.

## Discussion

In this study we investigated US and CECT findings of serologically proven tu-

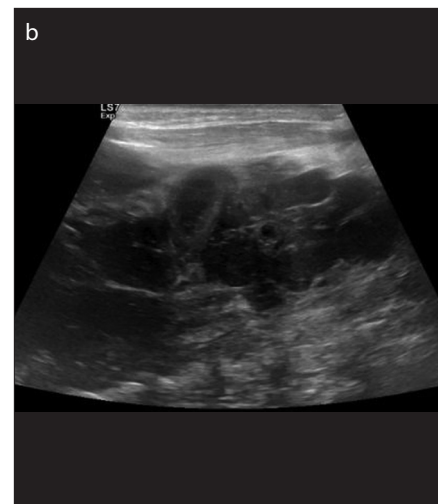


**Figure 1. a, b.** A 46-year-old woman presented with swelling on the left side of the neck. Gray scale US (a) shows enlarged level 2 lymph node, which is round and hypoechoic without echogenic hilum (arrows). Intranodal cystic necrosis (arrowhead) is seen. Longitudinal US (b) of the same patient shows multiple matted lymph nodes with internal hypoechoic areas consistent with necrosis on the left side of the neck. This patient was diagnosed with the glandular form of tularemia.

**Table 2.** US features of lymph nodes in tularemia patients

	n (%)
	n=48
Shape	
Oval	5 (10.4)
Round	43 (89.6)
Echogenic hilum	
Absent	44 (91.7)
Present	4 (8.3)
Nodal border	
Sharp	41 (85.4)
Irregular	7 (14.6)
Necrosis	38 (79.1)
Matting	11 (22.9)
US, ultrasonography.	

laremia patients. Prominent findings were level 2 and level 3 lymphadenopathy with cystic necrosis, matting, absence of calcification, oropharyngeal and retropharyngeal involvement, and neck abscess in tularemia patients.

Nodal neck masses are commonly encountered in daily clinical practice. Differential diagnosis of nodal neck masses is quite miscellaneous (congenital, infectious, inflammatory, neoplastic, and autoimmune). Upper respiratory tract infections, tuberculosis, lymph node metastases, and lym-



**Figure 2.** A 50-year-old woman with glandular tularemia. Contrast-enhanced CT shows typical tularemia lymph nodes with cystic necrosis (arrows) at left level 1 and 2. Additionally, enlarged lymph node (arrowhead) is seen at right level 2.

phoma are the main diseases that should be considered in the differential diagnosis in adults. When evaluating a patient with nodal neck mass, various factors should be considered, such as age, previous medical history, family history, habits, and concurrent disease. After a detailed anamnesis, complete head and neck examination with endoscopy, serologic tests, and radiologic imaging is crucial. US is the first-line imaging technique for this purpose because of its availability and cost-effectiveness. The role of US in evaluating cervical lymph

**Table 3.** Contrast-enhanced CT features of lymph nodes in tularemia patients

	n (%) n=42
Shape	
Oval	0 (0)
Round	42 (100)
Echogenic hilum	
Absent	41 (97.6)
Present	1 (2.4)
Nodal border	
Sharp	24 (57.1)
Irregular	18 (42.9)
Necrosis	41 (97.6)
Matting	22 (52.4)

CT, computed tomography.

nodes is well established. Different sonographic criteria have been described to differentiate benign from malignant cervical lymph nodes, such as size, shape, hilum, and border features (13). When US is combined with FNAC for the evaluation of cervical lymphadenopathy, the sensitivity, specificity, and accuracy are 89%–98%, 95%–98%, and 95%–97%, respectively (15). CECT is the modality of choice for defining accurate localization and extension of disease, relationship with the surrounding structures, and pre-surgery planning. CECT is also useful in patients with cervical lymph node metastases from unknown primary site for detecting primary tumor. Magnetic resonance imaging provides high soft-tissue contrast resolution for morphologic evaluation of lymph nodes and their relationships. Diffusion-weighted imaging can help differentiate benign from malignant lymph nodes (16).

The US features of cervical lymph nodes in tularemia patients were assessed as hypoechoic and round shape without echogenic hilum, which tend to show intranodal cystic necrosis (3). Our findings were in concordance with previous studies. However, these findings may be seen in tuberculous and malignant involvements, such as squamous cell carcinoma and papillary thyroid carcinoma metastasis (17, 18). In this study, a sharp nodal border was found in most cases. Although malignant nodes usually have sharp nodal borders, irregular nodal borders may be seen due to extracapsular spread of the tumor. Calcification within

**Table 4.** Frequency of surrounding structure involvement on contrast-enhanced CT

	n (%) n=42
Oropharyngeal inflammatory soft tissue	22 (52.4)
Retropharyngeal region	
Lymph node	2 (4.8)
Inflammatory soft tissue	2 (4.8)
Abscess+inflammatory soft tissue	4 (9.5)
Laryngeal involvement	2 (4.8)
Parotid preauricular involvement	13 (31)
Periorbital edema	4 (9.5)

CT, computed tomography.

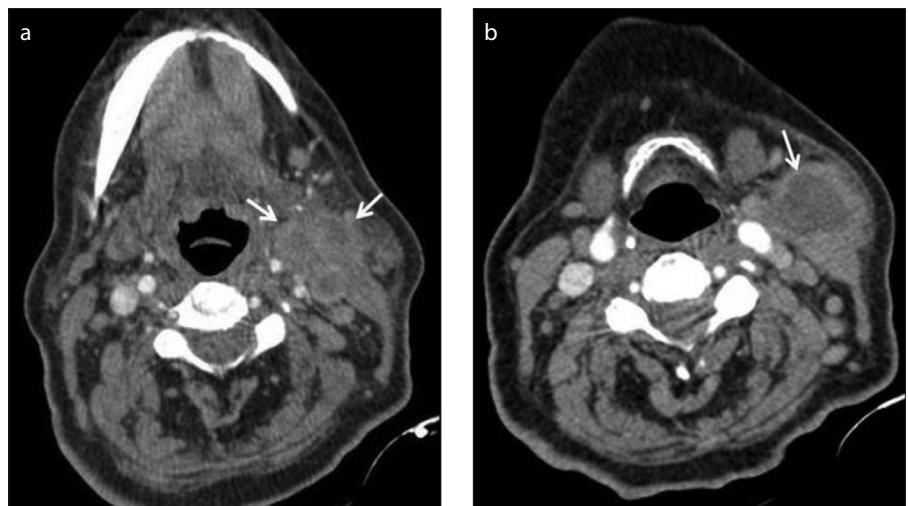


**Figure 3.** a, b. Contrast-enhanced CT (a) shows multiple matted enlarged lymphadenopathy (arrows) with intranodal cystic necrosis. Abscess formation (arrow) is seen near the sternocleidomastoid muscle at the more inferior level of the neck in the same patient (b).

lymph nodes is highly suggestive of metastases from medullary and papillary thyroid carcinoma (18). Remarkably, we did not encounter any calcification in lymph nodes on US or CECT in tularemia patients.

Although matting was also described in malignant and tuberculous nodes, it has not been previously described in tularemia (13, 19). Matting was seen in 22.9% and 52.4% patients on US and CECT, respectively. To the best of our knowledge, this is the first study that exhibits matting of lymph nodes in tularemia patients.

There are a few studies on CECT findings of tularemia (3, 11). In these studies, the clinical aspects of radiologic findings were evaluated. To the best of our knowledge our study is the largest CECT series of tularemia. In addition to the features of lymph nodes, we also defined oropharyngeal, retropharyngeal, laryngeal, parotid preauricular, and



**Figure 4.** A 45-year-old woman with oropharyngeal tularemia. Coronal reformatted CT image shows oropharyngeal inflammatory soft tissue (arrows) on the right side, which obliterates parapharyngeal fatty tissue. Lymphadenopathies with cystic necrosis (arrowhead) are seen at right level 2.



**Figure 5.** A 36-year-old woman with oropharyngeal tularemia. Sagittal reformatted CT image demonstrates retropharyngeal abscess (arrow), which was not visible on US.

periobital region involvements on CECT. In our study, oropharyngeal, retropharyngeal, laryngeal, parotid preauricular, and periobital region involvement were seen in 52.4%, 19.1%, 4.8%, 31%, and 9.5% of patients, respectively, on CECT. CECT should be used for identifying deep-lying lymph nodes and revealing their relationship with the surrounding structures, which is not possible with US. It is important to define the exact localization of disease and abscess for optimal drainage and decision of incision sites.

Tuberculosis and tularemia have similar imaging and cytopathologic findings (20, 21). The most common result of FNAC in this study was suppurative inflammation (72.4%). Multinucleated giant cells and granuloma formation were seen in 13.7% and 17% of patients, respectively. The same histopathologic features may be present in tuberculosis. Atmaca et al. (22) suggested that some tularemia patients may be misdiagnosed and treated for tuberculosis. Tularemia is rarely considered in the differential diagnosis of granulomatous inflammation in the absence of epidemiologic data. Streptomycin, which is used for treating tuberculosis, is also effective for patients with tularemia, but because of misdiagnosis, these patients are subjected to unnecessary long-term anti-tuberculosis therapy and its side effects. Therefore, it is important to be able to distinguish between tularemia and tuberculosis. Tuberculous adenitis is usually seen in the bilateral supraclavicular region and posterior triangle of the neck (23, 24), whereas level 2 and level 3 were the most frequently involved neck sites, and bilateral nodal involvement was

seen only in 17% of patients with tularemia in our study. Although pharyngeal and laryngeal tuberculosis can cause oropharyngeal, laryngeal, or retropharyngeal inflammatory soft tissue, extranodal head and neck tuberculosis is quite rare (25). In our study, oropharyngeal and retropharyngeal involvements were seen in 52% and 19% of patients, respectively. Considering the abovementioned findings, a serologic test (micro-agglutination test) can be conducted using serum samples, and tularemia can be diagnosed within two days. A definitive diagnosis of tuberculosis can only be made by culturing *Mycobacterium tuberculosis* from a specimen taken from the patient (sputum or biopsied tissue). Biopsy is an invasive procedure and diagnostic process may take a long time. Early diagnosis can prevent the formation of abscess and unnecessary long-term anti-tuberculosis therapy.

Antibiotherapy is the mainstay of treatment of tularemia. Ulu-Kilic et al. (3) reported that early treatment (within 21 days of the onset of symptoms) was associated with a significantly higher success rate. Treatment failure was observed more frequently (60%) in patients with nodal necrosis and abscess in the late phase of the infection. The current study revealed that longer duration of symptoms was associated with abscess formation, which is consistent with the literature (11). Surgical drainage is needed in the presence of abscess formation to shorten the recovery time. Occasionally, if enlarged and matted lymph nodes persist despite the antibiotherapy, surgical excision of lymph nodes may be necessary. It is important to determine intranodal necrosis, matting, and abscess formation and define the exact localization of disease by imaging methods for management of tularemia patients and decision of surgery.

The main limitation of our study is its retrospective design. Accordingly, some patients did not undergo both US and CECT examinations. Moreover, a relatively small number of cases showed FNAC results.

In conclusion, US and CECT are useful imaging modalities for diagnosis in tularemia patients. Tularemia should be considered in the presence of level 2 and level 3 lymph nodes with cystic necrosis, matting, no calcification, oropharyngeal and retropharyngeal involvement, and neck abscess, particularly in endemic areas.

#### Conflict of interest disclosure

The authors declared no conflicts of interest.

#### References

1. Tärnvik A, Berglund L. Tularemia. *Eur Respir J* 2003; 21:361–373. [CrossRef]
2. McCoy GW. A plague like disease of rodents. *Public Health Bull* 1911; 43:53–71.
3. Ulu-Kilic A, Gulen G, Sezen F, Kilic S, Sencan I. Tularemia in Central Anatolia. *Infection* 2013; 41:391–399. [CrossRef]
4. Akalin H, Helvacı S, Gedikoğlu S. Re-emergence of tularemia in Turkey. *Int J Infect Dis* 2009; 13:547–551. [CrossRef]
5. Gunnell MK, Lovelace CD, Satterfield BA, Moore EA, O'Neill KL, Robison RA. A multiplex real-time PCR assay for the detection and differentiation of *Francisella tularensis* subspecies. *J Med Microbiol* 2012; 61:1525–1531. [CrossRef]
6. Ulu Kilic A, Doganay M. Tularemia: A re-emerging disease. *Ankara Üniv Vet Fak Derg* 2013; 60:275–280. [CrossRef]
7. Ellis J, Oyston PC, Green M, et al. Tularemia. *Clin Microbiol Rev* 2002; 15:631–646. [CrossRef]
8. Erdem H, Ozturk-Engin D, Yesilyurt M, et al. Evaluation of tularemia courses: a multicentre study from Turkey. *Clin Microbiol Infect* 2014; 20:1042–1051. [CrossRef]
9. Nordahl SH, Hoel T, Scheel O, Olofsson J. Tularemia: a differential diagnosis in oto-rhino laryngology. *J Laryngol Otol* 1993; 107:127–129. [CrossRef]
10. Penn RL. *Francisella tularensis* (Tularemia). In: Mandell GL, Bennett JE, Dolin R eds. *Principles and practice of infectious diseases*. 6th ed. New York: Elsevier-Churchill Livingstone, 2005; 2674–2685.
11. Oztoprak N, Celebi G, Hekimoglu K, Kalaycioglu B. Evaluation of cervical computed tomography findings in oropharyngeal tularemia. *Scand J Infect Dis* 2008; 40:811–814. [CrossRef]
12. Chan JM, Shin LK, Jeffrey RB. Ultrasonography of abnormal neck lymph nodes. *Ultrasound Quarterly* 2007; 23:47–54. [CrossRef]
13. Ahuja AT, Ying M, Hoa SY, et al. Ultrasound of malignant cervical lymph nodes. *Cancer Imaging* 2008; 8:48–56. [CrossRef]
14. King AD, Tse GM, Ahuja AT, et al. Necrosis in metastatic neck nodes: diagnostic accuracy of CT, MR Imaging, and US. *Radiology* 2004; 230:720–726. [CrossRef]
15. Knappe M, Louw M, Gregor RT. Ultrasonography-guided fine-needle aspiration for the assessment of cervical metastasis. *Arch Otolaryngol Head Neck Surg* 2000; 126:1091–1096. [CrossRef]
16. Perrone A, Guerisi P, Izzo L, et al. Diffusion-weighted MRI in cervical lymph nodes: differentiation between benign and malignant lesions. *Eur J Radiol* 2011; 77:281–286. [CrossRef]
17. Ying M, Ahuja A. Sonography of neck lymph nodes. I. Normal lymph nodes. *Clin Radiol* 2003; 58:351–358. [CrossRef]
18. Ahuja A, Ying M. Grey-scale sonography in assessment of cervical lymphadenopathy: review of sonographic appearances and features that may help a beginner. *Br J Oral Maxillofac Surg* 2000; 38:451–459. [CrossRef]
19. Reshma VJ, Shihab AA, Abdulla M, Vadivazhagan, Issac JK. Characterization of cervicofacial lymph nodes - a clinical and ultrasonographic study. *J Clin Diagn Res* 2014; 8:ZC25–ZC28.
20. Ahuja A, Ying M. Sonography of neck lymph nodes. II. Abnormal lymph nodes. *Clin Radiol* 2003; 58:359–366. [CrossRef]

21. Yildirim S, Turhan V, Karadenizli A. et al. Tuberculosis or tularemia? A molecular study in cervical lymphadenitis. *Int J Infect Dis* 2014; 18:47–51. [\[CrossRef\]](#)
22. Atmaca S, Bayraktar C, Çengel S, Koyuncu M. Tularemia is becoming increasingly important as a differential diagnosis in suspicious neck masses: experience in Turkey. *Eur Arch Otorhinolaryngol* 2009; 266:1595–1598. [\[CrossRef\]](#)
23. Ahuja A, Ying M, Evans R, King W, Metreweli C. The application of ultrasound criteria for malignancy in differentiating tuberculous cervical adenitis from metastatic nasopharyngeal carcinoma. *Clin Radiol* 1995; 50:391–395. [\[CrossRef\]](#)
24. Vazquez E, Enriquez G, Castellote A. et al. US, CT, and MR imaging of neck lesions in children. *Radiographics* 1995; 15:105–122. [\[CrossRef\]](#)
25. Burrill J, Williams CJ, Bain G, Conder G, Hine AL, Misra RR. Tuberculosis: a radiologic review. *Radiographics* 2007; 27:1255–1273. [\[CrossRef\]](#)